

Functional Influence of the Pore Helix Glutamate in the KcsA K⁺ Channel

HoSook Choi and Lise Heginbotham

Department of Molecular Biophysics and Biochemistry, Yale University, New Haven, Connecticut 06520-8114

ABSTRACT The E71 residue is buried near the selectivity filter in the KcsA K⁺ channel and forms a carboxyl-carboxylate bridge with D80. We have investigated the importance of E71 by examining neutralization mutants at this position using biochemical and electrophysiological methods. E71 mutations differentially destabilize the detergent-solubilized tetramer; among them, the E71V neutralization mutant has a relatively subtle effect. The E71V channel displays electrical activity when reconstituted into planar lipid bilayers. In single channel recordings, the mutant retains K⁺/Na⁺ selectivity, and its conductance in the outward direction is unaltered. Some conduction properties are changed: inward conductance is increased. Our results show that the E71 side chain is not a primary determinant of ion selectivity or conduction in the wild-type channel, either directly or through the E71:D80 carboxyl-carboxylate bridge.

INTRODUCTION

The KcsA K⁺ channel provides a unique opportunity to study the molecular details of ion permeation in a highly selective channel. Structural studies confirm that selectivity is determined by the interaction of permeant ions directly with backbone carbonyl oxygen atoms from sequential residues of a segment known as the signature sequence (Doyle et al., 1998). The unique conformation of this segment arises from two sources: the glycine-rich primary sequence of the signature sequence and the architecture of the support scaffolding formed by surrounding protein (Doyle et al., 1998).

A key component of this scaffold is the pore helix located immediately adjacent to the signature sequence. In KcsA, the pore helix contains E71, the sole ionizable residue buried within the core of the protein. In the context of membrane proteins, where the low dielectric or the membrane environment increases their energetic burden, buried ionizable residues generally play critical roles in structure or catalysis (e.g., Zhukovsky and Oprian, 1989; Jiang et al., 2003a). The high-resolution structure of KcsA indicates that E71 interacts through a carboxyl-carboxylate linkage with D80 (Zhou et al., 2001). D80 is located at the outer mouth of the channel on the distal side of the signature sequence, and its side chain is accessible to the external solution. The crucial role of D80 in stabilizing the buried E71 side chain explains an earlier observation that neutralizing the D80 side chain severely compromises KcsA's oligomeric stability (Heginbotham et al., 1997).

Although E71 has not been examined using functional approaches, it has been the subject of numerous computational studies. These calculations show that, in its charged form, the E71 side chain dramatically affects the potential

energy profile within the selectivity filter, but that the E71 side chain is protonated in its most stable configuration (Guidoni et al., 1999; Roux et al., 2000; Ranatunga et al., 2001; Berneche and Roux, 2002); in these models, E71 forms a hydrogen bond with the D80 side chain.

In this study we use biochemical and electrophysiological approaches to examine how E71 influences the stability and function of the KcsA K⁺ channel. We find that neutralizing this residue does not influence ionic selectivity but does alter channel stability and single channel conductance.

MATERIALS AND METHODS

Materials

All chemicals were of reagent grade. 1-Palmitoyl-2-oleoyl phosphatidylethanolamine (POPE) and phosphatidylglycerol (POPG) were from Avanti Polar Lipids (Alabaster, AL). Dodecylmaltoside and 3-[(3-cholamidopropyl)dimethylammonio]-1-propanesulfonic acid (CHAPS) were from Anatrace (Maumee, OH). Nitrilotriacetic (NTA)-agarose Ni²⁺ affinity matrix was obtained from QIAGEN (Valencia, CA). *N*-methylglucamine (NMG) and Sephadex G-50 were obtained from Sigma (St. Louis, MO) and from Amersham Pharmacia Biotech (Uppsala, Sweden), respectively. The *Streptomyces lividans* K⁺ channel KcsA was modified with a hexahistidine tag added to the NH₂-terminus as previously described (Heginbotham et al., 1999).

Mutagenesis, purification, and reconstitution of KcsA

Site-directed mutagenesis was performed using the Quickchange mutagenesis kit (Stratagene, La Jolla, CA) and mutations were confirmed by DNA sequencing of the entire gene. Protein was expressed in *Escherichia coli* strains JM83 or DH-5 α and purified on Ni²⁺ affinity columns as previously described (Heginbotham et al., 1997). Briefly, cells were grown in Terrific Broth and protein expression was induced with anhydrotetracycline when the A550 reached 1.0. Cells were disrupted with either sonication or French press, and were collected by centrifugation at 100,000 \times *g* after first removing unbroken cells by high-speed centrifugation. Membranes were resuspended in buffer A (95 mM NaCl, 5 mM KCl, 50 mM 3-(*N*-morpholino)propanesulfonic acid (MOPS), pH 7), and protein was extracted with 15 mM dodecyl maltoside. Extract was incubated with Ni²⁺ affinity matrix in the presence of 40 mM imidazole. Purified protein was eluted in

Submitted October 31, 2003, and accepted for publication December 18, 2003.

Address reprint requests to Lise Heginbotham, Yale University, Dept. of Molecular Biophysics and Biochemistry, Bass 234, New Haven, CT 06520. Tel.: 203-432-9803; E-mail: lise.heginbotham@yale.edu.

© 2004 by the Biophysical Society

0006-3495/04/04/2137/08 \$2.00

400 mM imidazole. Purified protein was immediately reconstituted into liposomes as previously described (Heginbotham et al., 1999) by adding protein to a phospholipid mixture of 1-palmitoyl-2-oleoyl phosphatidylethanolamine and 1-palmitoyl-2-oleoyl phosphatidylglycerol (3:1 molar ratio), resuspended in 450 mM KCl, 10 mM HEPES, 4 mM *N*-methylglucamine, pH 7.4, and solubilized with 34 mM CHAPS, and then removing the CHAPS by gel filtration. Eluted liposomes were aliquoted and stored at -80°C for up to 2 months.

Protein biochemistry

Stability was assessed using standard SDS-PAGE with Laemmli buffers (Laemmli, 1970). Protein (6 μg per lane) was incubated under the indicated conditions of time and temperature, separated on a 12% gel, and visualized with Coomassie stain. When examining temperature stability, the Laemmli sample buffer was mixed with protein before incubation; for the time course assay, it was added just before loading the gel.

Single-channel recording

Single channel recordings of wild-type (wt) and mutant KcsA were performed in horizontal planar lipid bilayers as previously described (Heginbotham et al., 1999). Partitions were prepared from overhead transparency films; bilayers had capacitances of 20–60 pF. Electrodes were connected to *cis* and *trans* chambers by 2% agar salt bridges containing 200 mM KCl buffered at pH 7; selectivity measurements were made with an equivalent bridge containing Na^+ connected to the *trans* chamber. *Cis* and *trans* solutions were maintained at pH 7 and 4, respectively. With this pH configuration, active channels are oriented with cytoplasmic and extracellular surfaces facing the *trans* and *cis* solutions, respectively. The *cis* solutions contained the indicated concentration of K, and were made by using 10 mM 3-(*N*-morpholino)propanesulfonic acid, 4 mM KOH, and KCl to the indicated potassium concentration. *Trans* chambers were filled with solutions made with either 10 mM succinic acid, 4 mM KOH, or 10 mM K_2 succinate, and KCl added to the desired K^+ concentration. Voltages and currents use the standard electrophysiological convention with the *cis* chamber (extracellular solution) defined as zero voltage. Electrophysiological data were collected using an Axopatch 200B amplifier and Clampex software (v8.0 and v9.0, Axon Instruments, Burlingame, CA). Data were sampled at 10 kHz and filtered at 1–2-kHz bandwidth.

Kinetic modeling

The kinetic model shown in Fig. 7 A was evaluated using Matlab 6.5.1, with rate constants as follows: AB, CD, EF, and GH: $1 \times 10^8 \text{ s}^{-1}$; BA, DC, FE, and HG: $1 \times 10^9 \text{ s}^{-1}$; AC, BD, EG, and FH: $1 \times 10^9 \text{ s}^{-1}$; CA, DB, GE, and HF: $1 \times 10^9 \text{ M}^{-1} \text{ s}^{-1}$; BG and GB: $4 \times 10^9 \text{ s}^{-1}$; AE, BF, CG, and DH: $3 \times 10^8 \text{ M}^{-1} \text{ s}^{-1}$ (wt) or $1 \times 10^{10} \text{ M}^{-1} \text{ s}^{-1}$ (E71V); EA, FB, GC, and HD: $3 \times 10^9 \text{ s}^{-1}$ (wt) or $1 \times 10^{11} \text{ s}^{-1}$ (E71V). Transitions into and within the selectivity filter have equal voltage dependence. In voltage-dependent transitions, voltage dependence is partitioned evenly between forward and backward rates.

RESULTS

The unique architecture of the pore-lining signature sequence determines the basic properties of ionic selectivity and conduction in all K^+ channels. Several ionizable residues are prominently conserved in the adjacent regions (Fig. 1 A): in KcsA, E71 lies on the pore helix and is buried within the protein, whereas D80 is located at the outer mouth of the channel (Fig. 1 B). In eukaryotic channels, analogous flanking pairs of ionizable side chains are found solely among

A

	63	70	80	3
Shaker	PDAFWWAVVTMT	TVGYGDMTP		
KAT1	VTALYWSITTLT	TTGYGDFHA		
BK	WTCVYFLIVTMS	TVGYGDVYC		
SK1	LGAMWLISITFL	SIGYDMVP		
K_vAP	FDALWWAVVTAT	TVGYGDVVP		
MthK	TVSLYWTFVTTI	ATVGYGDYSP		
KcsA	PRALWWSV	E TAT TVGYG DLYP		
KirBac	VGAFFFSVETL	ATVGYGDMHP		
KIR 1.1	TS AFLFSL	ETQVTIGYGRFV		
KIR 2.1	TAAFLFSI	ETQTTIGYGRFCV		
KIR 3.1	PSAFLFFI	E TEATIGYGYRYI		
KIR 4.1	TGAFLFSL	ESQTTIGYGRFYI		

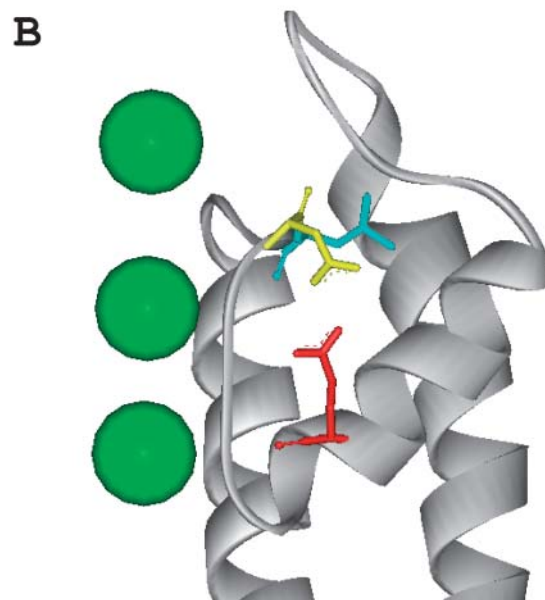


FIGURE 1 Conservation and disposition of E71 in K^+ channel pores. (A) Alignment of the region segment flanking the signature sequence (shown in gray), for a variety of K^+ channels (left); residue numbers correspond to those of KcsA. (B) The position of conserved residues within the context of the folded protein are shown mapped onto the extracellular half of a KcsA subunit. The E71 and D80 side chains are shown in red and yellow, respectively. The potassium ions (shown in green space-filling model) show the relative position of the conduction pore. (Primary sequences are from Medline entries: Shaker, M17211; *Arabidopsis thaliana* K^+ channel (KAT)1, M86990; high-conductance Ca^{2+} -activated K^+ channel (BK), M96840; small-conductance Ca^{2+} -activated K^+ channel (SK)1, U69883; KIR 1.1, X72341; KIR 2.1, X73052; KIR 3.1, U50964; and KIR 4.1, AF322631). Sequences of prokaryotic channels are from the following sources: K_v from *A. permix* (K_vAP; Ruta et al., 2003); MthK (Jiang et al., 2002a); KcsA (Schrempf et al., 1995); and *Burkholderia pseudomallei* K^+ channel (KirBac) (Durell and Guy, 2001)). Fig. 1 B was drawn using WebLab Viewer Pro (Molecular Simulations, San Diego, CA) from PDB file 1K4C.

two-transmembrane (2TM) K^+ channels; in members of the inward rectifier K^+ channel (KIR) family, residues equivalent to E71 and R81 (Fig. 1) have been proposed to form an

ionic bond critical in stabilizing the selectivity filter (Yang et al., 1997). But the primary sequences of the *Methanobacterium thermoautrophicum* K⁺ (MthK) channel and most 6TM channels indicate that such a bond is not an absolute requirement for selectivity in all channels, since many of these channels contain aliphatic residues at the sites equivalent to E71. The work presented here was motivated by the simple question: how does the buried E71 impact channel function in KcsA?

Mutations at position 71 affect oligomeric stability

We generated a group of point mutations at E71 that included aliphatic (Ile and Val) and polar (Gln and Met) side chains, as well as glycine. Each of the mutant proteins could be isolated from purified membranes after expression in *E. coli*, indicating that both membrane insertion and folding tolerate a broad diversity of residues at E71.

The mutant channels were next screened to assess their stability and function. Because fully assembled KcsA channel is relatively stable in detergent micelles, its oligomeric state is easily assessed using conventional SDS-PAGE (Heginbotham et al., 1997). Three of the E71 mutant channels (Gly, Ile, and Met) displayed no SDS-stable tetramer (data not shown). Two mutant channels, Gln and Val, did pass this screen and were subsequently examined for activity in planar lipid bilayers. The Gln mutant channel displays activity when reconstituted into bilayers, but channel openings are quite flickery. We focused instead on the Val mutant channel, which, as described in detail below, is much better behaved. Val is structurally unrelated to the native Glu but is commonly found at the analogous position in many 6TM channels (Fig. 1 A). The hydrophobic Val side chain certainly has very different packing interactions than the native Glu, leading us to wonder if it might induce subtle alterations of channel stability not detected in the original screen.

Fig. 2 A shows a thermal denaturation experiment in which both wild-type and E71V mutant protein have been incubated at the indicated temperatures for 30 min. Wild-type KcsA is remarkably stable; tetrameric protein is still apparent after treatment at 80°C. In contrast, the overwhelming majority of E71V protein is monomeric even at 60°C. Although the E71V mutation clearly affects the thermodynamics of oligomeric stability, denaturation is not reversible under these conditions (data not shown), and so our data cannot distinguish if the E71V mutation alters the final monomer/tetramer equilibrium or simply the kinetics of this association. Regardless, the finding that E71V alters stability raised a further practical concern: whether the E71V mutant channel might denature in the course of purification although solubilized in detergent micelles. We accordingly examined purified E71V protein at room temperature for evidence of time-dependent denaturation. No change was observed in the amount of tetramer over a 12-h period (Fig.

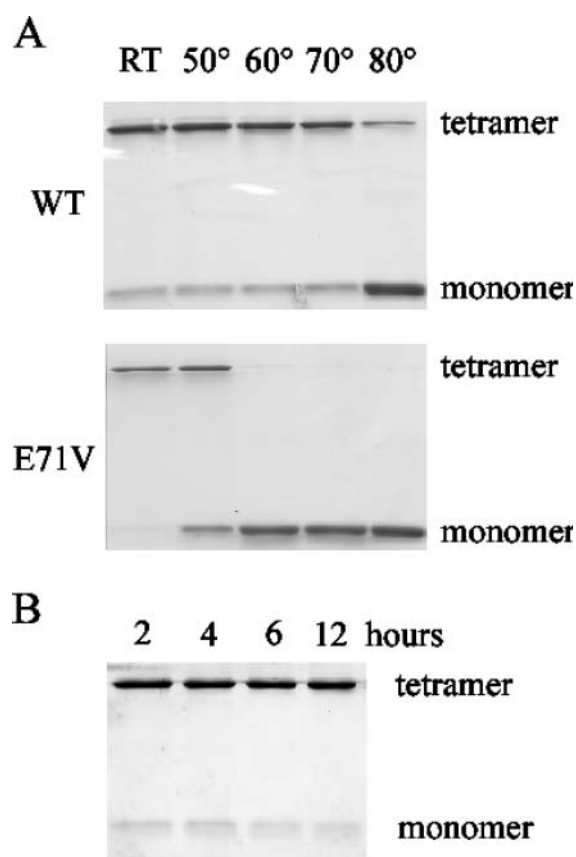


FIGURE 2 Oligomeric stability of E71V. (A) Coomassie-stained gels of purified wild-type and E71V mutant channels incubated at the indicated temperatures for 30 min. (B) E71V mutant protein was incubated at room temperature for the indicated period, separated with SDS-PAGE, and then visualized with Coomassie stain.

2 B), confirming that the protein is stable during the roughly 7 h required for its purification and reconstitution.

The E71V mutant has altered single channel conductance

Single channel studies of the wild-type KcsA channel almost exclusively examine the channel at positive potentials. This is simply because openings at positive voltages are well behaved, but the inward openings are quite flickery, as though contaminated by a fast, unresolved, gating process (Heginbotham et al., 1999).

The E71V mutation has a dramatic effect on inward conduction. The data illustrated in Fig. 3 were recorded in solutions of symmetric 200 mM K⁺, and focus on how the single channel current through E71V varies with voltage. Although the mutation has little effect on the magnitude of currents in the outward direction under these conditions, it has several obvious effects on inward currents. Firstly, the large inward openings in E71V are well defined, in contrast to the very noisy inward currents observed in the wild-type channel (Heginbotham et al., 1999; LeMasurier et al., 2001).

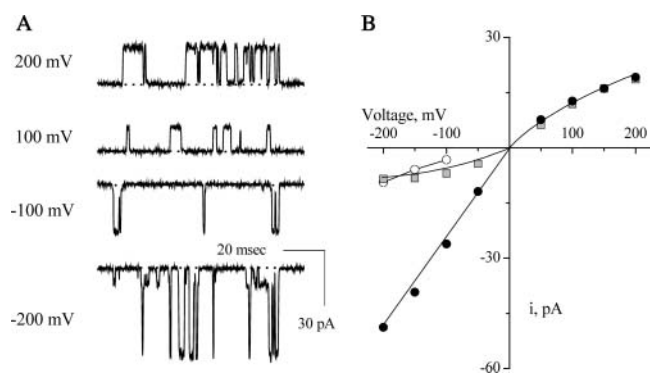


FIGURE 3 Single channel recordings from the E71V mutant channel. (A) Single channel currents were recorded at the indicated potentials in 200 mM symmetric K^+ , *cis* pH 7, *trans* pH 4. In this and subsequent figures the dotted line indicates the closed state. (B) Open channel current-voltage relationship for the main (open circle) and subconductance (solid circle) states of E71V are compared to that of the wild-type channel (shaded square). Data are the mean of 4–12 determinations; standard errors are smaller than symbols. Curves through data have no theoretical meaning.

Secondly, at nearly 240 pS, the chord conductance at -200 mV is much larger than that of wild-type KcsA, which, calculated from published data, is ~ 40 pS under the same ionic conditions (LeMasurier et al., 2001). As shown in Fig. 3 B, wild-type KcsA rectifies slightly in the outward direction. The increase in inward conductance seen in E71V, coupled with the fact that the outward currents are unaffected, results in pronounced inward rectification for the E71V mutant. Thirdly, E71V displays a prominent subconductance level, particularly at negative potentials (Fig. 3 A); this is not seen in comparable recordings from the wild-type channel (Heginbotham et al., 1999). At -200 mV, the magnitude of this subconductance is identical to that of the inward current in the wild-type channel, raising the possibility that the open state of the wild-type channel is analogous to that of the E71V subconductance. However the two diverge at less extreme potentials (Fig. 3 B) and, as will be discussed later, at higher potassium concentrations, indicating that inward conduction through the E71V subconductance state is not equivalent to that through the wild-type channel.

Although the majority of channels have the characteristics shown in Fig. 3, individual E71V mutant channels exhibit distinctive variation in both gating and conductance. Fig. 4 illustrates this range of behaviors with four recordings taken under identical conditions. A–C show the array of gating activity; channels can behave as shown in Fig. 3 (Fig. 4 A), be predominantly open (Fig. 4 B), or display an intermediate behavior (Fig. 4 C). In addition, the E71V mutant channel also has a second conductance mode, with a -200 -mV chord conductance of 160 pS, with characteristically long openings (Fig. 4 D). Since wild-type KcsA channels can also display variability in gating (E. Kutluay and L. Heginbotham, unpublished observation), we suspect that the different behaviors shown in Fig. 4 are probably not induced by the

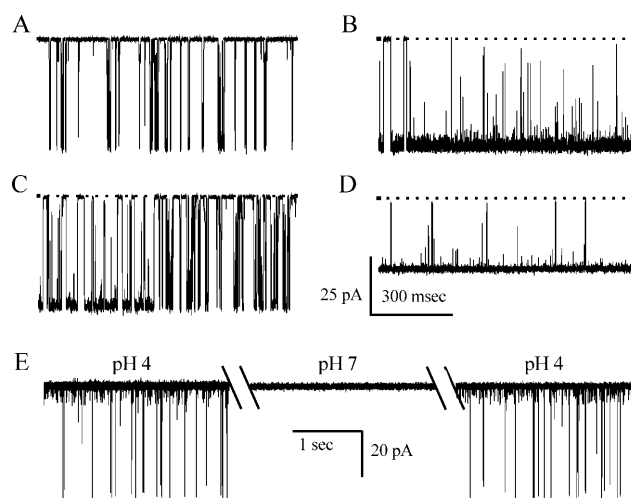


FIGURE 4 Gating characteristics of E71V. (A–C) Microscopic variability of E71V. Traces from three different E71V channels recorded under identical conditions at -200 mV in 200 mM symmetric K^+ , *cis* pH 7, *trans* pH 4. (D) pH sensitivity of E71V. Segments taken from a continuous single channel recording at -150 mV in 200 mM symmetric K^+ after perfusing the *trans* chamber with solutions at the indicated pH. The *cis* chamber was maintained at pH 7. Hatches indicate interruptions for perfusion.

E71V mutation per se, but rather that they are simply more pronounced in this mutant channel.

Throughout the rest of this article, we focus on channels behaving as in Fig. 4 A. This mode is the most prevalent and is easily identified and relatively stable. As shown in Fig. 4 E, this gating mode retains KcsA's characteristic pH sensitivity (Heginbotham et al., 1999). This latter characteristic allowed us to assure the orientation of the channel in all subsequent experiments by maintaining the extracellular and intracellular solutions at pH 7 and 4, respectively.

E71V retains K^+ selectivity under biionic conditions

The proximity of E71 to the selectivity filter, coupled with the structural constraints E71 forces on the selectivity filter through its interaction with D80, raises the question of whether neutralizing this side chain affects channel selectivity. Since currents carried by Na^+ are difficult to detect directly, selectivity for K^+ over Na^+ is typically evaluated under biionic conditions (Hille, 2001). In this case, the microscopic variability of the E71V mutant would seriously complicate interpretation of macroscopic recordings. Fortunately, the large conductance of the E71V mutant allows biionic measurements to be conducted at the single channel level.

Channels were fused and initially inspected in standard K^+ solutions (200 mM K^+ , pH 7 external); after establishing the gating and conductance mode of the incorporated channel, the internal solution was exchanged with 200 mM Na^+ , pH 4. Inward currents carried by K^+ were plainly visible at 0 mV (Fig. 5 A), indicating that the E71V mutant

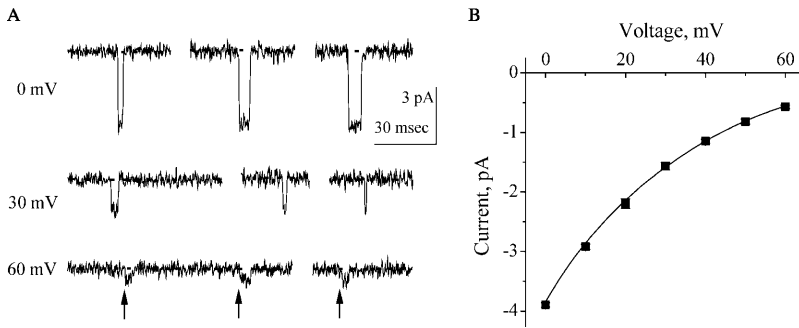


FIGURE 5 Selectivity of E71V under biionic conditions. (A) Raw currents were recorded with 200 mM Na_{int}⁺ and 200 mM K_{ext}⁺ at the indicated potentials. Traces at each potential are discontinuous. Arrows indicate the beginning of openings at -60 mV. (B) Open channel current-voltage relationship. Data are the mean from three determinations; mean \pm SE are smaller than symbols. Curve through data has no theoretical meaning.

channel retains its basic selectivity for K⁺ over Na⁺. The conductance of the channel decreased with depolarizing potentials (Fig. 5, A and B), but small inward openings could be discerned even at +60 mV. Openings at this potential are relatively brief and, at roughly 0.5 pA, are at the limit of our resolution given the noise inherent in the bilayer experiments. We examined a voltage range extending to +200 mV, but above +60 mV saw no clear fluctuations from baseline in either direction. We suspect this reflects a very high selectivity for K⁺ over Na⁺. (Although we cannot rigorously exclude the possibility that the channel simply fails to open under these conditions, it seems unlikely; channel openings are frequent at these potentials in symmetric K⁺, and channel activity is relatively unaffected by internal Na⁺ between 0 and +60 mV.)

The inward openings at 0 mV establish unambiguously that E71V is selective for K⁺ over Na⁺; the observation of current at +60 mV provides a minimal limit of >10:1 for the K⁺/Na⁺ permeability ratio. This value is actually higher than that established for wild-type KcsA, which is known to

be quite selective for K⁺ over Na⁺, under similar conditions (a minimal limit of $P_{K^+}/P_{Na^+} > 7:1$; LeMasurier et al., 2001).

E71V conductance-concentration relationship

Our initial examination of the current-voltage relationship in E71V suggested that the mutation altered inward conduction without changing currents in the outward direction. To confirm that this observation did not result from a coincidental choice of recording conditions, we examined how channel conductance changed as the K⁺ concentration was increased. Although the precise shape of the conductance-concentration relationship reflects complex details of the permeation process (Hille, 2001), the maximal conductance at high substrate concentration provides a simple means of probing for changes in the limiting throughput rate of the channel.

We studied the channel at concentrations ranging to 1.6 M (Fig. 6 A), measuring chord conductances at both +200 and -200 mV to permit direct comparisons with previously published data for the wild-type channel (LeMasurier et al., 2001).

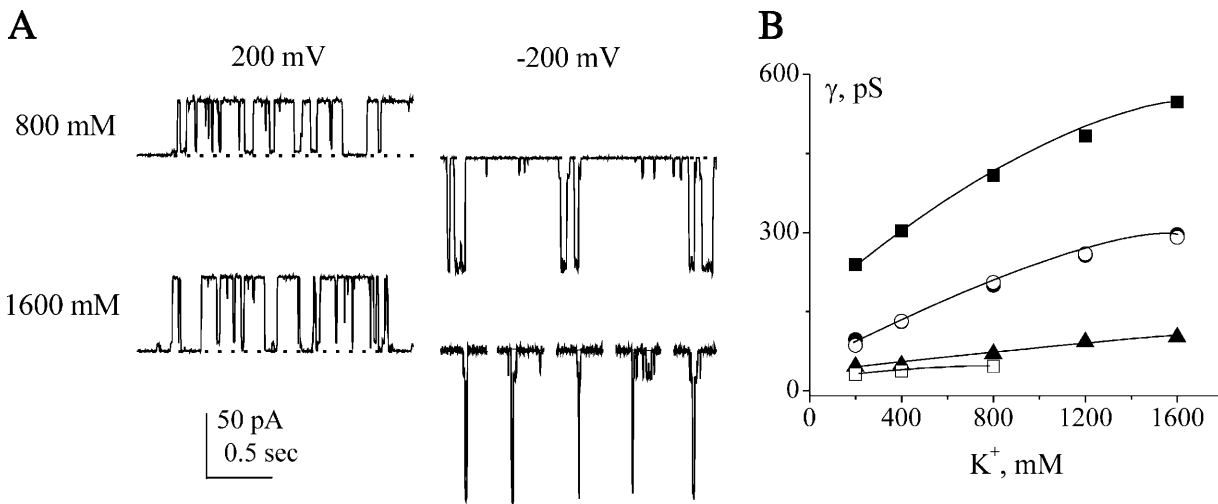


FIGURE 6 Conductance-concentration curves for E71V. (A) Single channel currents were recorded at either 200 or -200 mV at the indicated K⁺ concentrations. The traces shown at -200 mV in 1600 mM K⁺ are not continuous. (B) Chord conductances measured in this study for E71V (solid symbols) are compared with those previously determined for wild-type KcsA (open symbols; LeMasurier et al., 2001). Conductances were determined for main and subconductance states at -200 mV (square and triangle symbols, respectively) and at +200 mV (circle symbols). For data acquired at +200 mV, data from the wild-type channel lie directly under those from the E71V mutant, except for slight differences at 200 and 1600 mM K⁺. Symbols indicate means of 3-6 determinations; standard errors are smaller than the symbols.

There are differences in the magnitude of the conductances measured at these two voltages, but the overall shapes of the concentration-dependence curves are similar to each other and to that of the wild-type channel (Fig. 6B). The conductance of the E71V mutant shows the complex potassium dependence characteristic of KcsA. Over this concentration range, conductance is in a slow creep phase; although there is a hint of a plateau, the conductance does not actually reach full saturation at K^+ concentrations up to 1.6 M.

The E71V mutation has no effect on the +200-mV chord conductance over the entire K^+ range. At saturating K^+ , conductance is no longer constrained by the entry rate of ions to the channel but rather by the steps of the translocation process itself; these data indicate that the rate-limiting step in outward conduction is not affected by the E71V mutation.

In contrast, the E71V mutation increases the -200-mV chord conductance at all K^+ concentrations. Approaching 600 pS, the E71V conductance is nearly 10-fold larger than in wild-type KcsA and exceeds even the Ca^{2+} -activated K^+ channel, which saturates at roughly 400 pS (MacKinnon et al., 1989). In many potassium channels, conductance can be tuned by electrostatic focusing of permeant ions at the outer vestibules (MacKinnon et al., 1989; Nimigean et al., 2003). The effect of E71V is inconsistent with such a simple mechanism, since the mutation should then affect conductance at low ion concentrations, where entry to the pore is slow, but not at saturating K^+ concentrations. Instead, the E71V mutation is likely to affect the translocation steps of inward ion permeation.

The subconductance state seen at negative potentials saturates at ~100 pS. This is well above the 45-pS value previously reported for the sole conductance of the wild-type channel in the inward direction and is further evidence that these two do not represent equivalent conducting states. At high potassium concentrations, a small subconductance becomes apparent in the outward direction; we have not studied this in detail.

DISCUSSION

Ionizable residues play diverse and crucial roles in K^+ channel function. Residues located at the protein surface affect conduction through their effects on local ion concentration (MacKinnon et al., 1989; Nimigean et al., 2003), charged residues serve as the voltage sensors in the voltage-dependent K^+ (K_V) channels (Papazian et al., 1991; Jiang et al., 2003b), and in the KIR channels, a buried salt bridge is postulated to be critical for channel stability (Yang et al., 1997). Our experiments examine the importance of the buried ionizable residue in KcsA. The E71V neutralization mutant is well suited for this study, as this substitution mutes any electrostatic influence of the side chain and can form neither ionic nor hydrogen bonds.

Our examination of the E71V mutant channel yields two basic insights about the E71 side chain. Firstly, E71 is not

strictly required for channel function. The E71V mutant protein was sufficiently stable to withstand purification, which requires detergent solubilization, and displayed channel activity when reconstituted into lipid bilayers. Secondly, E71 is not required for K^+/Na^+ selectivity. In the *Shaker* K^+ channel, mutation of an immediately adjacent residue eliminates K^+/Na^+ discrimination (Heginbotham et al., 1994), and given its proximity to the selectivity filter, the E71 side chain might even have direct effects on ion permeation. These studies indicate that any such interactions between the E71 side chain and permeant ions are not a primary influence in dictating selectivity. Moreover, the physical constraint provided by the E71:D80 carboxyl-carboxylate bridge is not essential for either conduction or selectivity.

Role in channel stability

Although wild-type KcsA is a very stable tetramer, previous work has shown that the oligomer is easily disrupted by mutations in or adjacent to the selectivity filter (Heginbotham et al., 1997; Irizarry et al., 2002), including neutralization mutants of D80. Given the tight packing within this region, it is not particularly surprising that many mutations at E71 dramatically destabilized the tetramer. Our SDS-PAGE assay cannot distinguish the underlying cause: the mutations may disrupt folding of the monomer, assembly of the tetramer, or both. However, the finding that E71V is a relatively stable tetramer indicates that the E71:D80 interaction is not a primary determinant of oligomeric stability.

The E71V mutant protein displays a number of different functional behaviors. It adopts several open conformations, including three conductance levels (250 pS, 160 pS, and at least one small subconductance state) and two gating modes. It is not yet clear what structural differences underlie these functional polymorphisms. In the case of the *Shaker* K^+ channel, subconductance levels appear to reflect partial openings on the pathway to full activation (Zheng and Sigworth, 1997, 1998); the conductance levels of E71 may reflect similar transitional conformations. Because we have not studied this mutant in its native membrane, we do not know if the channel displays intrinsic heterogeneity or if this is a consequence of its purification and reconstitution. Although the E71V channel is reasonably amenable to single-channel studies, its variability may preclude macroscopic work.

Influence on permeation and blockade

Although E71 is not strictly necessary for a conducting pore, neutralization of this residue does have a clear, contained effect; it alters the inward conductance without affecting outward currents. Where physically might this mutation be felt? It is clear that the E71V neutralization need not result in large conformational changes: the MthK and *Aeropyrum pernix* K_V (K_{VAP}) structures overlay well with KcsA in this region (Jiang et al., 2002a, 2003a), and both of these

channels contain an aliphatic residue at E71. Since the properties of ion conduction are generally quite sensitive to perturbations of the selectivity filter, the finding that both outward current and selectivity remain unaltered suggests that the signature sequence itself has not undergone a radical structural rearrangement. Below we describe several of the possible explanations for the contained effect on inward conductance; these possibilities are not mutually exclusive, and we suspect that both are important in the E71V mutant.

First, as previously mentioned, inward currents through wild-type KcsA are very noisy, as though the channel is undergoing a very rapid gating that is not completely resolved by our recordings (Heginbotham et al., 1999). In contrast, currents through the main conductance state of the E71V channel are relatively well behaved, as though the channel assumes a stable open configuration. Thus the effect of E71V may be to slow the gating to reveal the true conductance state of KcsA. In this scenario, unresolved rapid gating would decrease the apparent conductance at all K⁺ concentrations, as we observed experimentally. The physical origin of such rapid gating is likely to be quite different from that of the slow, millisecond timescale, pH-dependent process. Given the location of E71, its mutation could easily affect gating occurring at the level of the selectivity filter.

Secondly, the E71V mutation may primarily affect the kinetic parameters of ion conduction itself; the following discussion considers one case in detail. Fig. 7 A shows a model for ion conduction through the KcsA channel that we have used to assess the effect of the E71V mutation. This model considers only the main conductance state, since we suspect that the subconductance state reflects an incompletely open channel that may have a very different permeation cycle. The limitations of rate theory models in examining I-V relationships are well documented (Miller, 1999; Nonner et al., 1999); our purpose in presenting this

model is simply to provide a foundation for an intuitive understanding of the effect of the E71V mutation. This model is based on the four-state permeation model developed by Nimigean and Miller (Nimigean et al., 2003) and reminiscent of others describing conduction through KcsA (Morais-Cabral et al., 2001; Berneche and Roux, 2003); we have expanded it to eight states to accommodate a consideration of the S0 site located within the outer vestibule. Ions enter the conduction pathway at the S0 site in the outer vestibule and then transit across the selectivity filter. Crystallographic studies indicate that there are four distinct binding sites within the filter and that typically two ions are bound simultaneously, at either sites 1 and 3 or 2 and 4 (Morais-Cabral et al., 2001). Conduction results principally from a concerted motion of the two ions between these two configurations. (For simplicity, we show only two of the four sites in the model.) Upon reaching the innermost site, S4, ions exit to the cavity, and then subsequently reach bulk solution.

Analysis of potassium channel crystal structures indicate that the vast majority of the electric field falls across the selectivity filter proper (Roux et al., 2000; Jiang et al., 2002b; Berneche and Roux, 2003); accordingly, we have assigned no voltage dependence to ion entry from the bulk to either the cavity or S0 site. Each transition associated with the filter, either from the vestibules to S1 or S4, or transitions between sites within the filter, have equivalent voltage dependence. The i-V curve of the wild-type channel has a characteristic plateau at negative potential voltages (Fig. 3) that suggests inward conduction is limited by a voltage-independent step. In our model these must correspond to the transfer of ions between bulk solution and either the cavity and S0 sites, since all other transitions are voltage-dependent. Fig. 7, B and C, show that simply by increasing the entry and exit rates from bulk solution to the S0 site, the model qualitatively accounts for both the change in recti-

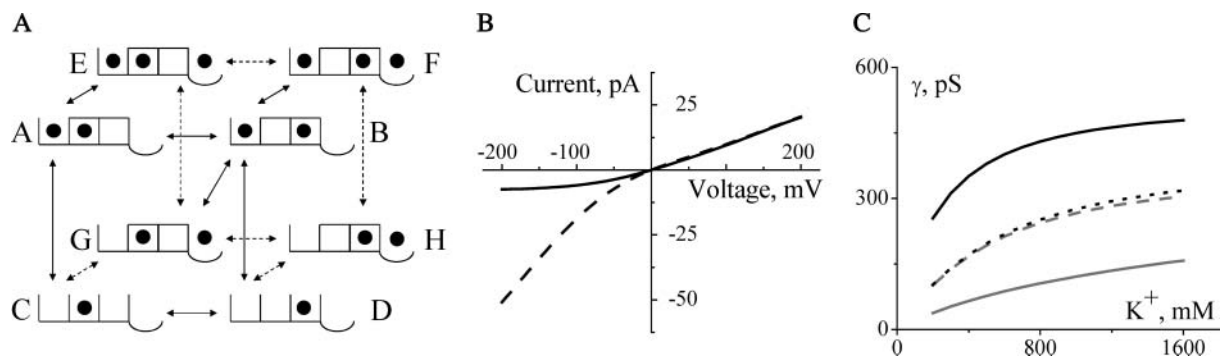


FIGURE 7 Model accounting for effect of E71V mutation. (A) Kinetic scheme showing the different conduction states. The open box on the left and semicircle on the right represent the cavity site and outer S0 sites, respectively. The four sites within the selectivity filter (sites S1–S4 from outside to inside) are assumed to be occupied pairwise and are depicted by the two closed boxes; (C and D) represent the conformations in which S2,S4 or S1,S3 are occupied, respectively. (B) Simulation of the current generated by model A with rate constants given in the Materials and Methods section. The solid line reflects CG and GC rates of $3 \times 10^8 \text{ M}^{-1} \text{ s}^{-1}$ and $3 \times 10^9 \text{ s}^{-1}$; changing these rates to $1 \times 10^{10} \text{ M}^{-1} \text{ s}^{-1}$ and $1 \times 10^{11} \text{ s}^{-1}$ yields the dashed line. (C) Simulation of chord conductances at -200 and $+200$ mV using model A and the rate constants given in the Materials and Methods section. The -200 -mV chord conductances for wild-type and E71V are shown with solid shaded and black lines, respectively; the $+200$ -mV chord conductances for wild-type and E71V are shown with black dotted and shaded dashed lines, respectively.

fication at the single channel level, as well as the general effect on the conductance-concentration curves. Outward current is unaffected by these rate changes over the entire range of $[K^+]$, as observed in our experiments (Fig. 7 B). In contrast, the inward current is dramatically increased at all potentials and no longer plateaus at extreme negative potentials. Consistent with our data, this model predicts that the inward conductance is larger than the outward conductance over the entire $[K^+]$ range (Fig. 7 C).

At a structural level, we suspect that the E71V mutation modestly affects the external entryway, leaving the conformation of the selectivity filter unaltered. We imagine that the functional changes result primarily from secondary effects through the D80 side chain. Since the E71 residue exists largely in a protonated state, its neutralization should not have long-range electrostatic effects. However with the disruption of the carboxyl-carboxylate bond in the E71V mutant, the D80 side chain is no longer stabilized in the protein core. Its influence is more pronounced at the outer surface, perhaps a consequence of slight rearrangements of the acidic side chains toward the outer vestibule. The absolute changes in rate constants reflect relatively small changes in free energy, roughly 2 kcal/mol, or less than the energy of a single hydrogen bond. Thus they need not reflect major conformational changes of the vestibule. Subtle alterations of the positions of the acidic side chains could slightly broaden the outer vestibule, enhancing access to S0 and thereby increasing both entrance and exit rates of ions from bulk solution to this site.

We are grateful to E. Kutluay for experimental assistance, C. Miller and C. Nimigeon for MatLab help, and E. Kutluay, C. Miller, J. Morais-Cabral, B. Roux, and W. Silverman for suggestions on the manuscript.

This work was supported by a grant from the National Institutes of Health (GM41747). L.H. is a Clare Boothe Luce Assistant Professor and Pew Scholar in the Biomedical Sciences. H.C. was supported by an Anderson Fellowship from Yale University.

REFERENCES

- Berneche, S., and B. Roux. 2002. The ionization state and the conformation of Glu-71 in the KcsA K^+ channel. *Biophys. J.* 82:772–780.
- Berneche, S., and B. Roux. 2003. A microscopic view of ion conduction through the K^+ channel. *Proc. Natl. Acad. Sci. USA.* 100:8644–8648.
- Doyle, D. A., J. Morais Cabral, R. A. Pfuetzner, A. Kuo, J. M. Gulbis, S. L. Cohen, B. T. Chait, and R. MacKinnon. 1998. The structure of the potassium channel: molecular basis of K^+ conduction and selectivity. *Science.* 280:69–77.
- Durell, S. R., and H. R. Guy. 2001. A family of putative K_{IR} potassium channels in prokaryotes. *BMC Evol. Biol.* 1:14.
- Guidoni, L., V. Torre, and P. Carloni. 1999. Potassium and sodium binding to the outer mouth of the K^+ channel. *Biochemistry.* 38:8599–8604.
- Heginbotham, L., M. LeMasurier, L. Kolmakova-Partensky, and C. Miller. 1999. Single streptomyces lividans K^+ channels: functional asymmetries and sidedness of proton activation. *J. Gen. Physiol.* 114:551–560.
- Heginbotham, L., Z. Lu, T. Abramson, and R. MacKinnon. 1994. Mutations in the K^+ channel signature sequence. *Biophys. J.* 66:1061–1067.
- Heginbotham, L., E. Odessey, and C. Miller. 1997. Tetrameric stoichiometry of a prokaryotic K^+ channel. *Biochemistry.* 36:10335–10342.
- Hille, B. 2001. *Ion Channels of Excitable Membranes*, 3rd ed. Sinauer Associates, Sunderland, MA.
- Irizarry, S. N., E. Kutluay, G. Drews, S. J. Hart, and L. Heginbotham. 2002. Opening the KcsA K^+ channel: tryptophan scanning and complementation analysis lead to mutants with altered gating. *Biochemistry.* 41:13653–13662.
- Jiang, Y., A. Lee, J. Chen, M. Cadene, B. T. Chait, and R. MacKinnon. 2002a. Crystal structure and mechanism of a calcium-gated potassium channel. *Nature.* 417:515–522.
- Jiang, Y., A. Lee, J. Chen, M. Cadene, B. T. Chait, and R. MacKinnon. 2002b. The open pore conformation of potassium channels. *Nature.* 417:523–526.
- Jiang, Y., A. Lee, J. Chen, V. Ruta, M. Cadene, B. T. Chait, and R. MacKinnon. 2003a. X-ray structure of a voltage-dependent K^+ channel. *Nature.* 423:33–41.
- Jiang, Y., V. Ruta, J. Chen, A. Lee, and R. MacKinnon. 2003b. The principle of gating charge movement in a voltage-dependent K^+ channel. *Nature.* 423:42–48.
- Laemmli, U. K. 1970. Cleavage of structural proteins during the assembly of the head of bacteriophage T4. *Nature.* 227:680–685.
- LeMasurier, M., L. Heginbotham, and C. Miller. 2001. KcsA: it's a potassium channel. *J. Gen. Physiol.* 118:303–314.
- MacKinnon, R., R. Latorre, and C. Miller. 1989. Role of surface electrostatics in the operation of a high-conductance Ca^{2+} -activated K^+ channel. *Biochemistry.* 28:8092–8099.
- Miller, C. 1999. Ionic hopping defended. *J. Gen. Physiol.* 113:783–787.
- Morais-Cabral, J. H., Y. Zhou, and R. MacKinnon. 2001. Energetic optimization of ion conduction rate by the K^+ selectivity filter. *Nature.* 414:37–42.
- Nimigeon, C. M., J. S. Chappie, and C. Miller. 2003. Electrostatic tuning of ion conductance in potassium channels. *Biochemistry.* 42:9263–9268.
- Nonner, W., D. P. Chen, and B. Eisenberg. 1999. Progress and prospects in permeation. *J. Gen. Physiol.* 113:773–782.
- Papazian, D. M., L. C. Timpe, Y. N. Jan, and L. Y. Jan. 1991. Alteration of voltage-dependence of *Shaker* potassium channel by mutations in the S4 sequence. *Nature.* 349:305–310.
- Ranatunga, K. M., I. H. Shrivastava, G. R. Smith, and M. S. Sansom. 2001. Side-chain ionization states in a potassium channel. *Biophys. J.* 80:1210–1219.
- Roux, B., S. Berneche, and W. Im. 2000. Ion channels, permeation, and electrostatics: insight into the function of KcsA. *Biochemistry.* 39:13295–13306.
- Ruta, V., Y. Jiang, A. Lee, J. Chen, and R. MacKinnon. 2003. Functional analysis of an archaeobacterial voltage-dependent K^+ channel. *Nature.* 422:180–185.
- Schrempf, H., O. Schmidt, R. Kummerlin, S. Hinnah, D. Muller, M. Betzler, T. Steinkamp, and R. Wagner. 1995. A prokaryotic potassium ion channel with two predicted transmembrane segments from *Streptomyces lividans*. *EMBO J.* 14:5170–5178.
- Yang, J., M. Yu, Y. N. Jan, and L. Y. Jan. 1997. Stabilization of ion selectivity filter by pore loop ion pairs in an inwardly rectifying potassium channel. *Proc. Natl. Acad. Sci. USA.* 94:1568–1572.
- Zheng, J., and F. J. Sigworth. 1997. Selectivity changes during activation of mutant *Shaker* potassium channels. *J. Gen. Physiol.* 110:101–117.
- Zheng, J., and F. J. Sigworth. 1998. Intermediate conductances during deactivation of heteromultimeric *Shaker* potassium channels. *J. Gen. Physiol.* 112:457–474.
- Zhou, Y., J. H. Morais-Cabral, A. Kaufman, and R. MacKinnon. 2001. Chemistry of ion coordination and hydration revealed by a K^+ channel-Fab complex at 2.0 Å resolution. *Nature.* 414:43–48.
- Zhukovsky, E. A., and D. D. Oprian. 1989. Effect of carboxylic acid side chains on the absorption maximum of visual pigments. *Science.* 246:928–930.